PADOVA UNIVERSITY PRESS

Dolomites Research Notes on Approximation

Special issue of the "Seminari Padovani di Analisi Numerica 2018" (SPAN2018), Volume 11 · 2018 · Pages 3–10

Hopf bifurcation analysis of the fast subsystem of a polynomial phantom burster model

Iulia Martina Bulai[a] · Morten Gram Pedersen[b]

Communicated by Emma Perracchione

Abstract

Phantom bursters were introduced to explain bursting electrical activity in β-cells with different periods. We study a polynomial version of the phantom bursting model. In particular we analyse the fast subsystem, where the slowest variable is assumed constant. We find the equilibrium points of the fast subsystem and analyse their stability. Furthermore an analytical analysis of the existence of Hopf bifurcation points and the stability of the resulting periodics is performed by studying the sign of the first Lyapunov coefficient.

1 Introduction

The phantom bursting model was introduced to describe the episodic bursting of the pancreatic β-cells, where active phases are interspersed by silent ones. The model is characterised by two slow and two fast variables with the two slow variables having very different time scales [1].

In this paper we focus on the analysis of the fast subsystem model where the slowest of the two slow variables is considered constant, and thus can be used as a bifurcation parameter as made by Pernarowski and DeVries for the model with two fast and one slow variable in the Liénard form, [5, 2]. Here we want to show that a polynomial, minimal, phantom burster model can reproduce results obtained with the biophysical phantom burster model introduced in [9], with the advantage that it is easier to study analytically.

In Section 2 we introduce the complete polynomial phantom bursting model, and then pass to the fast subsystem model in Section 3. We analyse the existence of the equilibrium points and their stability. Furthermore we focus on the possible Hopf bifurcation (HB) points and the stability of the emerging periodic solutions by computing and analysing the sign of the first Lyapunov coefficient. We end the paper with conclusions.

2 The polynomial mathematical model

The polynomial version of the phantom bursting model as introduced in [6] is obtained after nondimensionalization and scaling of the system of four first-order equations introduced in [1], so called phantom bursting model. This model consist of a subset of fast variables that govern spiking during the active phase of a burst, and slow negative feedback to switch the spiking on and off. The fast variables are the membrane potential of the β-cell and the fast K^+ current activation variable, respectively. The first slow variable has a small time constant of a few seconds while the second one has a time constant more than a minute.

The transformation of the phantom burster model reduces the number of the parameters and simplifies the equations allowing an analytical analysis of the system. This transformation was made as in [12] for the Sherman-Rinzel-Keizer model, the burster model with two fast variables and a slow one. The model reads (here and in the following over-dots indicate time derivatives)

$$\begin{aligned} &\ddot{u} + F(u)\dot{u} + G(u) + \rho_z z_1 + z_2 + \frac{h_1(u) - z_1}{\tau_1} + \frac{h_2(u) - z_2}{\tau_2} = 0, \\ &\dot{z_1} = \frac{h_1(u) - z_1}{\tau_1}, \\ &\dot{z_2} = \frac{h_2(u) - z_2}{\tau_2}, \end{aligned} \tag{1}$$

where u is the transformed β-cell membrane potential, z_1 and z_2 are slow variables with z_1 faster than z_2, τ_1 is the z_1 time

[a]Department of Information Engineering, University of Padova, via Gradenigo, 6/B, 35131, Padova, Italy. Member of the research group GNCS of INdAM, email: bulai@dei.unipd.it

[b]Department of Information Engineering, and Department of Mathematics "Tullio Levi-Civita", University of Padova. Via Gradenigo, 6/B, 35131, Padova, Italy, email pedersen@dei.unipd.it

constant and τ_2 of z_2 respectively and

$$\begin{aligned} F(u) &= a\left[(u-\hat{u})^2-\eta^2\right], \\ G(u) &= u^3-3(u+1), \\ h_i(u) &= \beta_i(u-u_{\beta_i}), \quad i=1,2. \end{aligned} \tag{2}$$

The functions $F(u)$, $G(u)$ and $h_i(u)$, $i=1,2$ have biological interpretations related to the different ionic currents and channel conductances present in the phantom burster model introduced in [1].

The model (1) is equivalent to a system of four ODEs

$$\begin{aligned} \dot{u} &= v, \\ \dot{v} &= -F(u)v-G(u)-\rho_z z_1-z_2-\frac{h_1(u)-z_1}{\tau_1}-\frac{h_2(u)-z_2}{\tau_2}, \\ \dot{z_1} &= \frac{h_1(u)-z_1}{\tau_1}, \\ \dot{z_2} &= \frac{h_2(u)-z_2}{\tau_2}. \end{aligned} \tag{3}$$

Equating to zero the right hand side of (3) we get the equilibrium point $E=(\bar{u},0,h_1(\bar{u}),h_2(\bar{u}))$, with $\bar{u}$ the root of the cubic

$$-u^3+(3-\rho_z\beta_1-\beta_2)u+(3+\rho_z\beta_1u_{\beta_1}+\beta_2u_{\beta_2})=0. \tag{4}$$

To study the roots of (4) we analyse the sign of the discriminant

$$\Delta=4(3-\rho_z\beta_1-\beta_2)^3-27(3+\rho_z\beta_1u_{\beta_1}+\beta_2u_{\beta_2})^2, \tag{5}$$

in particular for

- $\Delta>0$: the equation (4) will have three distinct real roots
- $\Delta<0$: the equation (4) will have a single real root
- $\Delta=0$: the equation (4) will have a multiple root, and all of its roots are real.

The polynomial model with two slow variables was analysed by Griffiths and Pernarowski [7, 4], who obtained further results regarding the analysis of the complete system (3), a slow-subsystem and an averaged fast-subsystem. In contrast to the present work, they considered both z_1 and z_2 as slow variables, whereas in the following z_1 will be included in the fast subsystem.

3 The fast subsystem

To analyse the polynomial version of the phantom burster model in the space of parameters we will assume constant the slowest variable, z_2. It will be used as a bifurcation parameter in the same fashion made by Pernarowski [5], [3] and DeVries in [2]. The system to study becomes

$$\begin{aligned} \dot{u} &= v, \\ \dot{v} &= -F(u)v-G(u)-\rho_z z_1-z_2-\frac{h_1(u)-z_1}{\tau_1}, \\ \dot{z_1} &= \frac{h_1(u)-z_1}{\tau_1}. \end{aligned} \tag{6}$$

Following the same idea as for the complete model we compute the equilibrium of the fast subsystem (6), $E_*=(\bar{u},0,h_1(\bar{u}))$, with $\bar{u}$ the root of

$$P(u)=-u^3+(3-\rho_z\beta_1)u+(3+\rho_z\beta_1u_{\beta_1}-z_2)=0. \tag{7}$$

The discriminant of $P(u)$ is

$$\Delta=4(3-\rho_z\beta_1)^3-27(3+\rho_z\beta_1u_{\beta_1}-z_2)^2. \tag{8}$$

The inequality $\Delta>0$ (the case of three distinct real roots of $P(u)=0$), is satisfied if and only if

$$3+\rho_z\beta_1u_{\beta_1}-2\left(\frac{|3-\rho_z\beta_1|}{3}\right)^{\frac{3}{2}}<z_2<3+\rho_z\beta_1u_{\beta_1}+2\left(\frac{|3-\rho_z\beta_1|}{3}\right)^{\frac{3}{2}}. \tag{9}$$

Solving $P(u)=0$ we get $z_2=\gamma(u)$, where $\gamma(u)$ is a cubic curve of the shape

$$\gamma(u)=-u^3+u(3-\rho_z\beta_1)+3+\rho_z\beta_1u_{\beta_1}.$$

The curve $\gamma(u)$ is represented in Figure 1. It is divided in upper (Z_U), middle (Z_M) and lower (Z_L) branch by the right knee (K_R) and the left one (K_L) respectively.

Equating to zero $\gamma'(u)$ one get the two roots

$$u_L=-\sqrt{\frac{3-\rho_z\beta_1}{3}} \quad \text{and} \quad u_R=\sqrt{\frac{3-\rho_z\beta_1}{3}},$$

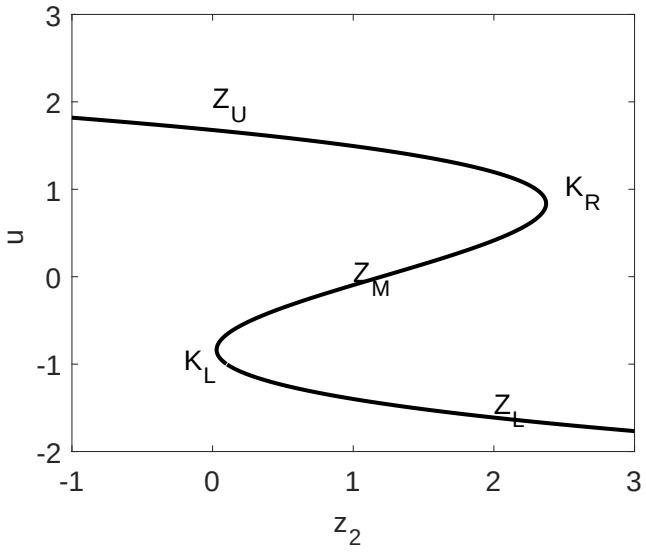

Figure 1: The curve $\gamma(u)$ is divided in upper (Z_U), middle (Z_M) and lower (Z_L) branch by the the right knee (K_R) and the left one (K_L) respectively.

which are real for $3-\rho_z\beta_1>0$. The abscissas of the left and right knee, K_L and K_R, are

$$\begin{aligned} z_{2,L} &= \gamma(u_L)=3+\rho_z\beta_1 u_{\beta_1}-2\left(\frac{|3-\rho_z\beta_1|}{3}\right)^{\frac{3}{2}} \quad \text{and} \\ z_{2,R} &= \gamma(u_R)=3+\rho_z\beta_1 u_{\beta_1}+2\left(\frac{|3-\rho_z\beta_1|}{3}\right)^{\frac{3}{2}}, \end{aligned}$$

the same expressions obtained solving $\Delta=0$ in (8) for z_2. From (9) we see that for z_2 between $z_{2,L}$ and $z_{2,R}$ there are 3 roots, and only one root to the left of $z_{2,L}$ and to the right of $z_{2,R}$. If $3-\rho_z\beta_1\le 0$ then there is always only one root $\bar{u}$.

3.1 Stability analysis of the critical points

To study the stability of the equilibrium points of the fast subsystem (6) we compute the Jacobian matrix

$$J=\begin{bmatrix} 0 & 1 & 0 \\ -G'(u)-\dfrac{\beta_1}{\tau_1} & -F(u) & -\rho_z+\dfrac{1}{\tau_1} \\ \dfrac{\beta_1}{\tau_1} & 0 & -\dfrac{1}{\tau_1} \end{bmatrix} \tag{10}$$

and evaluate it at $E_*=(\bar{u},0,h_1(\bar{u}))$. From the Routh-Hurwitz criteria

$$det(J-\lambda)=\lambda^3+c_1\lambda^2+c_2\lambda+c_3=0 \tag{11}$$

has three roots with negative real part, thus E_* is stable, iff

$$c_1>0, \quad c_3>0 \quad \text{and} \quad c_1c_2>c_3 \tag{12}$$

hold, where

$$\begin{aligned} c_1 &= F(\bar{u})+\frac{1}{\tau_1} \\ c_2 &= \frac{F(\bar{u})}{\tau_1}+G'(\bar{u})+\frac{\beta_1}{\tau_1} \\ c_3 &= \frac{G'(\bar{u})}{\tau_1}+\frac{\beta_1\rho_z}{\tau_1}. \end{aligned} \tag{13}$$

For a deeper analysis in the parameter space we use the fact that

$$\gamma'(u)=-3u^2+3-\rho_z\beta_1=-\frac{c_3}{\tau_1}.$$

Since $\tau_1>0$, analysing the sign of $\gamma'(u)$ will give us information about the sign of c_3. Without losing generality from now on we will assume $a>0$, $\hat{u}>\eta$, $\hat{u}-\eta\le u_L$ and $\hat{u}-\eta\ge u_R$. The cases where this hypothesis does not hold can be obtained in a similar way as done below. Studying $\gamma'(u)$'s behavior we get

(i) $\gamma'(u) < 0$, $(c_3 > 0)$, for values of $u < u_L$. Here two sub cases can be distinguished

- **(a)** $F(u) > 0$ $(u < \hat{u} - \eta)$, $c_1 > 0$: If $c_2 > 0$ all the coefficients of the characteristic polynomial (11) are positive while the coefficients of $det(-J + \lambda)$ have alternate signs, thus the eigenvalues have all negative real parts and the equilibrium points are stable. Notice that in this case if $c_1c_2 - c_3 = 0$ a HB arise. Otherwise if $c_2 < 0$ two of the eigenvalues will have positive real parts and the remaining one negative real part, the equilibrium points are unstable.
- **(b)** $F(u) < 0$ $(\hat{u} - \eta < u < u_L)$: $c_1 < 0$ two eigenvalues with positive real part and one with negative real part for both cases $c_2 < 0$ and $c_2 > 0$, the equilibrium points are unstable.

(ii) $\gamma'(u) = 0$, $(c_3 = 0)$, $u = u_L$ that corresponds to a saddle node bifurcation point. In fact the characteristic polynomial (11) has at least one variation in the signs of the coefficients (the same holds for the $det(-J + \lambda)$) thus is has an eigenvalue with positive real part, one with negative real part and one null.

(iii) $\gamma'(u) > 0$, $(c_3 < 0)$, for values of $u_L < u < u_R$, which corresponds to unstable saddle node points. In fact the characteristic polynomial (11) has at least one variation in the signs of the coefficients (the same holds for the $det(-J + \lambda)$) thus it has an eigenvalue with positive real part and the remaining two with negative real part.

(iv) $\gamma'(u) = 0$, $(c_3 = 0)$, $u = u_R$, that corresponds to a saddle node bifurcation point, same results as for point (ii).

(v) $\gamma'(u) < 0$, $(c_3 > 0)$, for values of $u > u_R$, as for case (i), two sub cases are possible

- **(a)** $F(u) > 0$ $(u > \hat{u} + \eta)$, $c_1 > 0$: same as for (ia).
- **(b)** $F(u) < 0$ $(u_R < u < \hat{u} + \eta)$: same as for (ib).

Table 1 summarizes the signs of the real parts of the three eigenvalues of (11).

Table 1: An overview of the stability analysis of the fast-subsystem equilibria.

Case	Subcases	$Re(\lambda)$	Equilibrium points
(i)	(a)	$---$	Stable equilibrium points
	(b)	$++-$	Unstable equilibrium points
(ii)		$+-0$	Saddle Node Bifurcation point
(iii)		$+--$	Unstable Saddle Node points
(iv)		$+-0$	Saddle Node Bifurcation point
(v)	(a)	$---$	Stable equilibrium points
	(b)	$++-$	Unstable equilibrium points

3.2 Hopf Bifurcation existence

In this section we will analyse the existence and the stability of the Hopf bifurcation of the fast subsystem (6). Conditions for $det(J - \lambda) = \lambda^3 + c_1\lambda^2 + c_2\lambda + c_3 = 0$ to have a pair of pure imaginary roots are $c_2 > 0$ and $c_3 - c_1c_2 = 0$.

To find values of u at which a HB occur, we solve $c_3 - c_1c_2 = 0$, i.e.,

$$\frac{G'(\bar{u})}{\tau_1} + \frac{\beta_1\rho_z}{\tau_1} - \left(F(u) + \frac{1}{\tau_1}\right)\left(\frac{F(u)}{\tau_1} + G'(u) + \frac{\beta_1}{\tau_1}\right) = 0,$$

which is equivalent to find the intersection points between $F(u)$ and $H(u)$, where

$$F(u) = a\left[(u - \hat{u})^2 - \eta^2\right], \tag{14}$$

$$H(u) = \frac{\beta_1\rho_z\tau_1 - \beta_1}{1 + \tau_1^2 c_2}. \tag{15}$$

To show that at least one root of $c_3 - c_1c_2 = 0$ exists we analyse $F(u)$ and $H(u)$ separately.

- The analysis of $F(u)$:
  $F(u)$ is a parabola of vertex $(\hat{u}, -a\eta^2)$. If $a > 0$, $F(u)$ is convex, otherwise is concave. From now on we will assume positive values of a. Furthermore $(\hat{u} \pm \eta, 0)$ are intersection points with the x axis while $(0, \hat{u}^2 - \eta^2)$ is an intersection point with the y axis. We will assume $\hat{u} \neq \eta$.
- The analysis of $H(u)$:
  $H(u)$ in (14) can be written as

$$H(u) = \frac{\beta_1\rho_z\tau_1 - \beta_1}{u^2(\tau_1 a + 3\tau_1^2) - u(2\tau_1 a\hat{u}) + (1 + \tau_1 a\hat{u}^2 - \tau_1 a\eta^2 - 3\tau_1^2 + \beta_1\tau_1)}. \tag{16}$$

a) $Dom H(u) = \left\{u \in \mathbb{R} \mid s_1u^2 - s_2u + s_3 \neq 0\right\}$, with s_1, s_2 and s_3 defined as the coefficients of the polynomial in the denominator of $H(u)$ in (16). The roots

$$u_{1,2} = \frac{s_2 \mp \sqrt{s_2^2 - 4s_1s_3}}{2s_1}$$

satisfy $u_1 < 0$ and $u_2 > 0$ and are two vertical asymptotes, in fact

$$\lim_{u \to u_1^{\pm}} H(u) = \pm sign(\beta_1\rho_z\tau_1 - \beta_1)\infty$$

and

$$\lim_{u\to u_2^{\pm}} H(u) = \mp sign(\beta_1\rho_z\tau_1-\beta_1)\infty.$$

b) $\lim_{u\to\pm\infty} H(u) = 0^{sign(\beta_1\rho_z\tau_1-\beta_1)}$, i.e., the x axis ($y=0$) is an horizontal asymptote.
c) No symmetries.
d) No intersection with x axis.
e) Intersection with y axis at $(0, y_*)$ with

$$y_* = \frac{\beta_1\rho_z\tau_1-\beta_1}{(1+\tau_1 a\hat{u}^2-\tau_1 a\eta^2-3\tau_1^2+\beta_1\tau_1)}.$$

f) Local max/min of $H(u)$: $\left(\frac{\tau_1 a\hat{u}}{\tau_1 a+3\tau_1^2}, \frac{\beta_1\rho_z\tau_1-\beta_1}{1+\tau_1 a\hat{u}^2-\tau_1 a\eta^2-3\tau_1^2+\beta_1\tau_1}\right)$, depending on the sign of the ordinate.

Considering the analysis above and excluding all the degenerate cases, remaining in the real case, $F(u)$ and $H(u)$ intersect in at most four points, which are HB points if the inequality $F(u)+\tau_1 G'(u)+\beta_1 > 0$ holds ($c_2(u) > 0$). Notice that the two asymptotes $u_{1,2}$ are the roots of $1+\tau_1^2 c_2$, which means that two of the four intersection points are HB points. A graphical representation of the intersection points between $F(u)$ and $H(u)$ can be seen in Figure 2, with the parameters values chosen properly.

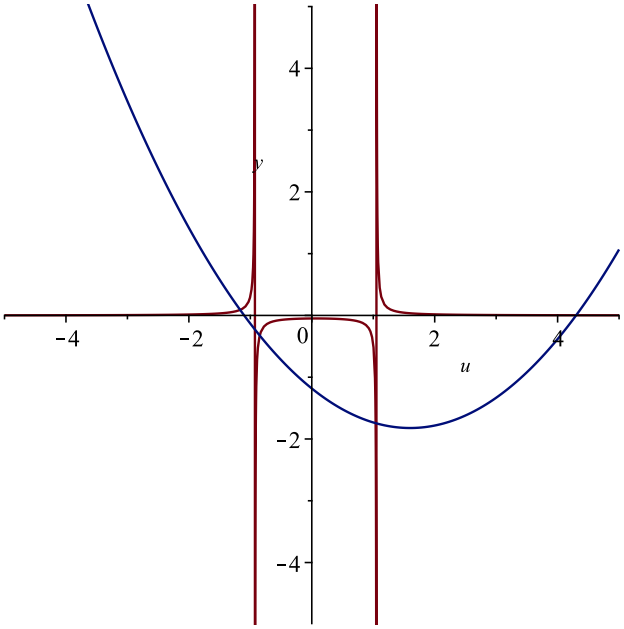

Figure 2: The intersection points between the parabola $F(u)$ and $H(u)$. The left most point and the right most one are HB points.

3.3 Hopf Bifurcation criticality

As was shown previously choosing an appropriate set of parameters can lead to the existence of at least one HB point. Assuming that the fast subsystem has an HB, the characteristic polynomial $det(J-\lambda)=0$ evaluated at $E_*(u_{HB}, 0, h_1(u_{HB}))$, with u_{HB} the intersection point between $F(u)$ and $H(u)$ such that $c_2(u_{HB}) > 0$, has two imaginary complex roots $\lambda_{1,2} = \pm i\omega_0$ and a real one λ_3,

$$det(J-\lambda) = \lambda^3 - \lambda_3\lambda^2 + \omega_0^2\lambda - \lambda_3\omega_0^2.$$

This implies that

$$\lambda_3 = -\left(F(u)+\frac{1}{\tau_1}\right) \quad \text{and} \quad \omega_0 = \pm\sqrt{\frac{F(u)}{\tau_1}+G'(u)+\frac{\beta_1}{\tau_1}}. \tag{17}$$

In order to analyse the criticality of the HB, (i.e. to determine the stability of the emerging limit cycle), we can compute the first Lyapunov coefficient $l_1(0)$ of the restricted system on the center manifold at the critical parameter value [8]. If $l_1(0) < 0$, the bifurcation is supercritical and a unique stable limit cycle bifurcates from the equilibrium point, otherwise if $l_1(0) > 0$, the bifurcation is subcritical. Next we will describe how the first Lyapunov coefficient of system (6) can be computed. For more details see Chapter 3 of [8].

Step 1: Since our equilibrium point is not the origin, introducing the new variables

$$\tilde{v} = v-\bar{v}, \quad \tilde{u} = u-\bar{u} \quad \text{and} \quad \tilde{z_1} = z_1 - h(\bar{z_1}) \tag{18}$$

with $\bar{v}$, $\bar{u}$ and $\bar{z_1}$ the values at equilibrium, the new system obtained is

$$\dot{x} = Jx + R(x),$$

with

$$x = \begin{bmatrix} \tilde{u} \\ \tilde{v} \\ \tilde{z_1} \end{bmatrix}, \quad R(x) = \begin{bmatrix} 0 \\ \tilde{u}\tilde{v}(2a\hat{u} - 2a\bar{u}) - 3\bar{u}\tilde{u}^2 - a\tilde{v}\tilde{u}^2 - \tilde{u}^3 \\ 0 \end{bmatrix}$$

and J the Jacobian matrix (10). From now on for simplicity we change the variable names $\tilde{u} \to u$, $\tilde{v} \to v$ and $\tilde{z_1} \to z_1$. As seen before J has a pair of complex eigenvalues $\lambda_{1,2} = \pm i\omega_0$ and a real one λ_3 as defined in (17). Using the expression of ω_0 in (17), J_{21} can be written equivalently $J_{21} = -\omega_0^2 + \frac{F(u)}{\tau_1}$, while the other elements of the Jacobian matrix remain as in (10).

Step 2: We need to compute the eigenvectors, q and p, of J for the eigenvalues $\lambda_{1,2} = \pm i\omega_0$, so that $Jq = i\omega_0 q$ and $J^t p = -i\omega_0 p$

$$q \sim \begin{pmatrix} 1 \\ i\omega_0 \\ \dfrac{\beta_1(1 - i\omega_0\tau_1)}{1 + \tau_1^2\omega_0^2} \end{pmatrix}, \quad p \sim \begin{pmatrix} F(u) - i\omega_0 \\ 1 \\ \dfrac{(\tau_1\rho_z - 1)(-1 - i\tau_1\omega_0)}{1 + \tau_1^2\omega_0^2} \end{pmatrix}.$$

To achieve the proper normalization $\langle p, q\rangle = \bar{p_1}q_1 + \bar{p_2}q_2 = 1$, one can take, for example

$$q = \begin{pmatrix} 1 \\ i\omega_0 \\ \dfrac{\beta_1(1 - i\omega_0\tau_1)}{1 + \tau_1^2\omega_0^2} \end{pmatrix}, \quad p = \frac{1}{A}\begin{pmatrix} F(u) - i\omega_0 \\ 1 \\ \dfrac{(\tau_1\rho_z - 1)(-1 + i\tau_1\omega_0)}{1 + \tau_1^2\omega_0^2} \end{pmatrix},$$

where

$$A = \frac{2\tau_1^2\omega_0^2 F(u)}{1 + \tau_1^2\omega_0^2} + i\frac{2\omega_0(1 + F(u))}{1 + \tau_1^2\omega_0^2}.$$

Step 3: Let us now write $R(x)$ in terms of multilinear functions $B(x, y)$ and $C(x, y, z)$

$$R(x) = \frac{1}{2}B(x, x) + \frac{1}{6}C(x, x, x) + O(\| x \|^4),$$

with x^t, y^t and $z^t \in \Re^3$,

$$B_i(x, y) = \sum_{j,k=1}^{3} \frac{\partial^2 R_i(\xi)}{\partial\xi_j\partial\xi_k}|_{\xi=0} x_j y_k, \quad i = 1, 2, 3$$

and

$$C_i(x, y, z) = \sum_{j,k,l=1}^{3} \frac{\partial^3 R_i(\xi)}{\partial\xi_j\partial\xi_k\partial\xi_l}|_{\xi=0} x_j y_k z_l, \quad i = 1, 2, 3.$$

$$B(x, y) = \begin{pmatrix} 0 \\ 2a(\hat{u} - \bar{u})(x_1y_2 + x_2y_1) - 6\bar{u}x_1y_1 \\ 0 \end{pmatrix},$$

$$C(x, y, z) = \begin{pmatrix} 0 \\ -2[a(x_2y_1z_1 + x_1y_1z_2 + x_1y_2z_1) + 3x_1y_1z_1] \\ 0 \end{pmatrix}.$$

Step 4: We want to compute $l_1(0)$ as was made in [8]

$$\begin{aligned} l_1(0) \quad = \quad & \frac{1}{2\omega_0} Re\big[\langle p, C(q, q, \bar{q})\rangle - 2\langle p, B\left(q, J^{-1}B(q, \bar{q})\right)\rangle + \\ & \langle p, B\left(\bar{q}, (2i\omega_0 I - J)^{-1}B(q, q)\right)\rangle\big]. \end{aligned} \tag{19}$$

This formula does not require a preliminary transformation of the system into its eigenbasis, and it expresses $l_1(0)$ using original, linear, quadratic and cubic terms, assuming that only the critical (ordinary and adjoint) eigenvectors of the Jacobian matrix are known. I is the identity matrix and $(\cdot)^{-1}$ represent the inverse matrix.

Step 5: We start by computing $B(q, q)$, $B(q, \bar{q})$, $C(q, q, \bar{q})$

$$B(q, q) = \begin{pmatrix} 0 \\ 4a(\hat{u} - \bar{u})i\omega_0 - 6\bar{u} \\ 0 \end{pmatrix}, \quad B(q, \bar{q}) = \begin{pmatrix} 0 \\ -6\bar{u} \\ 0 \end{pmatrix} \quad \text{and}$$

$$C(q,q,\bar{q}) = \begin{pmatrix} 0 \\ -2(ai\omega_0+3) \\ 0 \end{pmatrix}$$

and we conclude with computing $B\left(q, J^{-1}B(q,\bar{q})\right)$ and $B\left(\bar{q}, (2i\omega_0 I - J)^{-1}B(q,q)\right)$

$$B\left(q, J^{-1}B(q,\bar{q})\right) = \begin{pmatrix} -\dfrac{36\bar{u}^2}{G'(u)+\beta_1\rho_z} + \dfrac{12a(\hat{u}-\bar{u})\bar{u}i\omega_0}{G'(u)+\beta_1\rho_z} \\ 0 \end{pmatrix} \quad \text{and}$$

$$B\left(\bar{q}, (2i\omega_0 I - J)^{-1}B(q,q)\right) = \begin{pmatrix} M\left[2a(\hat{u}-\bar{u})\left(-2\omega_0^2 + \dfrac{i\omega_0}{\tau_1}\right) - 6\bar{u}\left(2i\omega_0 + \dfrac{1}{\tau_1}\right)\right] \\ 0 \end{pmatrix}$$

with

$$M = \frac{4a(\hat{u}-\bar{u})i\omega_0 - 6\bar{u}}{3Det(J) - 6i\omega_0^3} \quad \text{and} \quad Det(J) = -\frac{\beta_1\rho_z}{\tau_1} + \frac{G'(\bar{u})}{\tau_1}.$$

Step 5: Once we have $B(q,q)$, $B(q,\bar{q})$, $C(q,q,\bar{q})$, $B\left(q, J^{-1}B(q,\bar{q})\right)$ and $B\left(\bar{q}, (2i\omega_0 I - J)^{-1}B(q,q)\right)$, $l_1(0)$ the first coefficient of Lyapunov (19) can be found. We remind that $\langle\cdot,\cdot\rangle$ is the scalar product in $\mathbb{C}^2$. We will not report here the whole expression of $l_1(0)$, since we need only to evaluate its sign. Hence, it is enough to implement the formula in a mathematical software.

3.4 Numerical simulations

The numerical simulations were made with AUTO [10] as implemented in XPPAUT [11] and with Matlab. A set of parameters was found such as to have two HBs, one supercritical on the upper branch of the $\gamma(u)$ curve and a second one, subcritical, on the lower branch respectively, as in [9]. Figure 3 shows the obtained bifurcation diagram of the fast subsystem (7) with respect to z_2,.

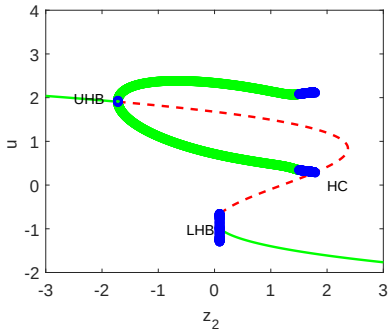

Figure 3: The bifurcation diagram of the fast subsystem (7) with respect to z_2. Green continuous line represent the stable equilibrium points while the dashed red line represent the unstable equilibrium points. The max and min of the stable limit cycles emerging from the upper HB are represented with green dots, while unstable periodics are indicated in blue. On the middle branch a homoclinic point (HC) is present. The parameter values are: $\hat{u} = 1.5$, $\eta = 0.4$, $a = 0.25$, $\beta_1 = 0.9$, $u_{\beta_1} = -2$, $\tau_1 = 120$ and $\rho_z = 1$.

In Figure 4 are represented the three solutions in time of the complete system (1), in particular from left to the right the transformed membrane potential u and the two slow variables z_1 and z_2, respectively.

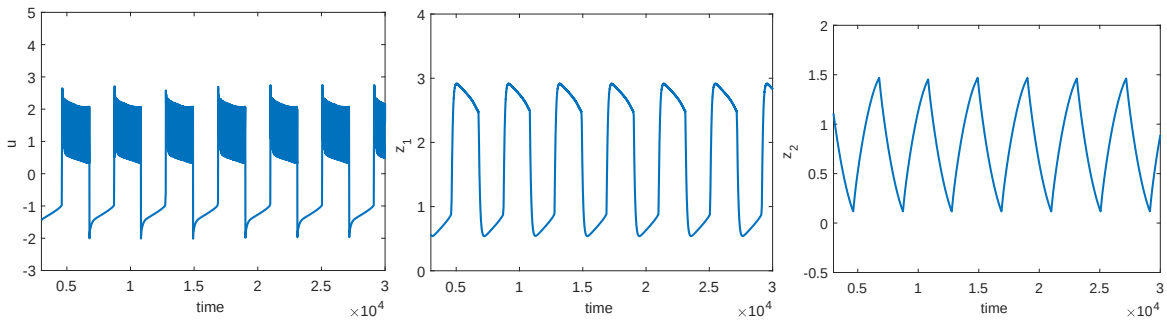

Figure 4: From left to the right the transformed membrane potential u and the two slow variables z_1 and z_2, of the complete system (1), respectively. The parameter values are: $\hat{u} = 1.5$, $\eta = 0.4$, $a = 0.25$, $\beta_1 = 0.9$, $u_{\beta_1} = -2$, $\tau_1 = 120$, $\rho_z = 1$, $u_{\beta_2} = -0.5$, $\beta_2 = 1.8$ and $\tau_2 = 3000$.

4 Conclusions

Assuming constant the slowest of the two slow variables of the polynomial phantom bursting model we get a three dimensional fast subsystem. Our analysis is different from the original analysis of phantom bursting [1, 6] where both z_1 and z_2 are treated as parameters, and the fast subsystem is two dimensional, effectively reducing the analysis to traditional bursting as in [2, 5]. The equilibrium points of the three dimensional fast subsystem were found and an analysis of their stability was made. The scenario found in [9], where two HBs can arise, a supercritical HB and a subcritical one respectively, is also found for the polynomial version of the phantom bursting model. In particular the method used to analyse the stability of the HBs points is the one introduced in Kuznetsov [8], where the sign of the first Lyapunov coefficient is analysed.

The analytical findings are confirmed by numerical simulations, in particular we found a set of parameter values for which two HBs can arise for the fast subsystem. The trajectories in time of the complete system were computed numerically, and here once more can be seen the different time scales of the variables, in particular the transformed membrane potential u is the faster one while z_1 and z_2 the slowest, with z_1 faster than z_2.

Acknowledgement
This work has been partially supported by the University of Padova, Strategic Research Project "DYCENDI", and Research Project SID (BIRD179302), to MGP. The research of IMB has been partially supported by "Finanziamento GNCS Giovani Ricercatori 2018/2019".

References

[1] R. Bertram, J. Previte, A. Sherman, T. A. Kinard, L. S. Satin. The Phantom Burster Model for Pancreatic β-Cells. *Biophysical Journal*, 79(6):2880–2892, 2000.

[2] G. de Vries. Multiple Bifurcations in a Polynomial Model of Bursting Oscillations. *J. Nonlinear Sci.*, 281(8), 1998.

[3] M. Pernarowski. Fast and Slow Subsystems for a Continuum Model of Bursting Activity in the Pancreatic Islet. *SIAM Journal on Applied Mathematics*, 58(5):1667–1687, 1998.

[4] R. E. Griffiths, M. Pernarowski. Return Map Characterizations for a Model of Bursting with Two Slow Variables. *SIAM Journal on Applied Mathematics*, 66(6):1917–1948, 2008.

[5] M. Pernarowski. Fast Subsystem Bifurcations in a Slowly Varying Liénard System Exhibiting Bursting. *SIAM Journal on Applied Mathematics*, 54(3):814–832, 1994.

[6] M. G. Pedersen. Phantom bursting is highly sensitive to noise and unlikely to account for slow bursting in β-cells: Considerations in favor of metabolically driven oscillations. *Journal of Theoretical Biology*, 248(2):391–400, 2007.

[7] R. E. Griffiths. RETURN MAP CHARACTERIZATIONS OF SINGULAR SOLUTIONS FOR A MODEL OF BURSTING WITH TWO SLOW VARIABLES. *PhD thesis*, 2003.

[8] Y. A. Kuznetsov. Elements of Applied Bifurcation Theory. *Springer-Verlag New York*, 1995.

[9] R. Bertram, J. Rhoads, W.P. Cimbora. A Phantom Bursting Mechanism for Episodic Bursting. *Bulletin of Mathematical Biology*, 70(7), 2008.

[10] E. J. Doedel and B. E. Oldeman. AUTO-07P : Continuation and Bifurcation Software for Ordinary Differential Equations. *Technical report, Concordia University Montreal, Canada*, 2012.

[11] B. Ermentrout. Simulating, Analyzing, and Animating Dynamical Systems: A Guide to XPPAUT for Researchers and Students. *Editor: Society for Industrial and Applied Mathematics*, (31 marzo 2002).

[12] M. Pernarowski and R. M. Miura and J. Kevorkian. The Sherman-Rinzel-Keizer Model for Bursting Electrical Activity in the Pancreatic β-Cel. *Lecture Notes in Biomathematics*, 34–54, 1990.